ISSN: 2710-0588

Research on Fuzzy PID Compliant Grinding Control Based on DBO Algorithm Optimization

Wei Wei, Wenguo Huo

Tianjin University of Technology and Education, Tianjin, China

Abstract

In order to achieve the requirements of high precision, fast response and low overshoot in the robot grinding process. An active compliant actuator at the end of the robot is designed, and a fuzzy PID constant force control method based on dung beetle optimizer (DBO) optimization is proposed. The force and gas flow model of the compliant actuator are analyzed, and the mathematical model of the actuator is established. On the basis of fuzzy PID algorithm, the fuzzy PID parameters optimized by DBO algorithm are adopted. The simulation system model is established by MATLAB, and the performance of PID control, fuzzy PID control and fuzzy PID control method optimized by DBO algorithm is compared. The simulation results show that the fuzzy PID control based on DBO algorithm has faster response speed, reaches stability in 0.5s, no overshoot, and the system is more stable.

Keywords

Grinding, Compliance control, Fuzzy PID, Dung beetle optimizer.

1. Introduction

Grinding still uses traditional manual methods due to the numerous challenges associated with grinding and polishing, including extremely strict requirements for the precision and stability of robot positioning and control of contact pressure [1-2]. Using industrial robots for grinding and polishing involves the robot's end making rigid contact with the workpiece, resulting in specific contact pressure. The complex surface topography of the workpiece makes real-time contact pressure adjustments unfeasible. Therefore, maintaining constant contact pressure and ensuring compliance during the process is a key issue in grinding and polishing operations.

Currently, corresponding actuators and control systems are designed according to the working scenario to achieve control of grinding and polishing contact force. Due to the difficulty in controlling the response speed and stability of the control system, enhancing the stability of grinding pressure and increasing the response speed of compliant polishing actuators are key to achieving compliant grinding and polishing[3].

2. Structural Design and System Modeling

2.1. Compliant grinding actuator structural design

The compliant grinding and polishing actuator uses a cylinder as the power element. The gas source supplies air, which is regulated by an electro-proportional valve to control the gas flow, thereby managing the internal pressure of the cylinder and producing a stable polishing contact pressure. The pressure sensor provides feedback on the contact pressure, and the controller adjusts the opening of the electro-proportional valve based on the feedback value to regulate the pressure output, achieving closed-loop control of the polishing contact pressure. The working principle is shown in Figure 1.

ISSN: 2710-0588

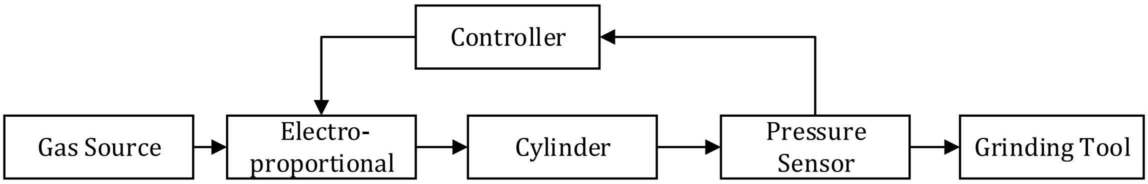

Figure 1. Working principle of the compliant grinding and polishing actuator

The performance of the compliant polishing actuator has a direct impact on the efficiency and accuracy of the polishing process. It is required to have a compact design, easy disassembly, reliable connections, and minimal friction in the relative movement parts to improve response speed. According to these requirements, the structure of the compliant polishing actuator is illustrated in Figure 2.

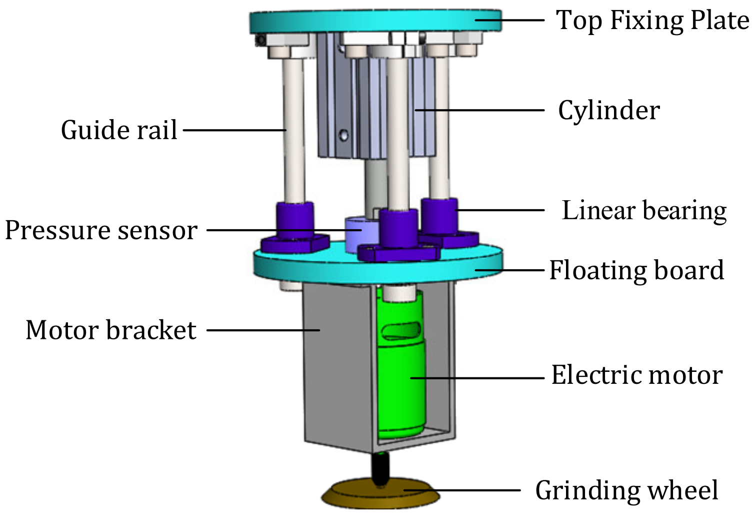

Figure 2. Structural design of the compliant polishing actuator

2.2. Modeling of the compliant polishing actuator system

The air circuit of the compliant grinding and polishing actuator is shown in Figure 3. The air source provides power for the entire device. The upper computer sends a voltage signal according to the set polishing pressure, and the electro-proportional valve controls the cylinder pressure based on the signal magnitude to generate the polishing contact pressure. The pressure-reducing valve provides a certain level of pressure to enhance system stability.

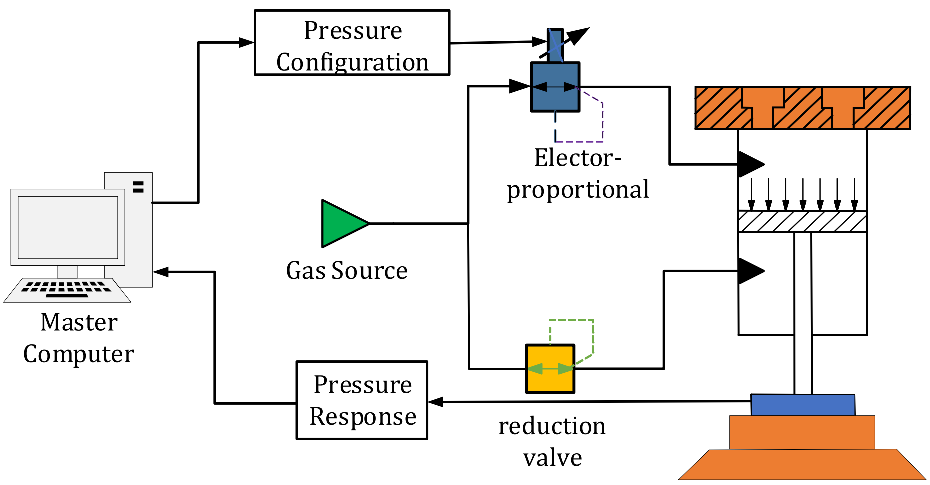

Figure 3. Air circuit of the compliant grinding and polishing actuator

ISSN: 2710-0588

The flow rate of gas through the electro-proportional valve depends on the pressure at the inlet and outlet and the spool opening area. The Sanvile flow formula [4] provides:

$$q = \begin{cases} \dfrac{C_v A_v P_u}{\sqrt{T}} \sqrt{\dfrac{k}{R_g}\left(\dfrac{2}{k-1}\right)} \sqrt{\left(\dfrac{P_d}{P_u}\right)^{\frac{2}{k}} \left(\dfrac{P_d}{P_u}\right)^{\frac{k+1}{k}}} & \dfrac{P_d}{P_u} > C \\ \dfrac{C_v A_v P_u}{\sqrt{T}} \sqrt{\dfrac{k}{R_g}\left(\dfrac{2}{k-1}\right)^{\frac{k+1}{k-1}}} & 0 \le \dfrac{P_d}{P_u} \le C \end{cases} \tag{1}$$

In the formula, q represents the gas flow rate through the electro-proportional valve; P_u is the inlet pressure; P_d is the outlet pressure; A_v is the effective opening area of the electro-proportional valve;k is the adiabatic coefficient; C_v is the throttling parameter of the electro-proportional valve; T is the absolute temperature; R_g is the ideal gas constant; C is set to 0.518.

The contact pressure during polishing does not need to be excessive, and the pressure at the outlet of the electro-proportional valve is relatively low, so the second form of equation (1) meets the condition.

Assuming that the inlet pressure and temperature of the electro-proportional valve remain constant, the flow through the valve is only related to the spool opening area, which in turn depends on the input voltage, thus controlling the outlet pressure. Linearization near the zero point yields the incremental flow model of the electro-proportional valve:

$$\Delta q = K_1 \Delta u + K_2 \Delta p_{dv} \tag{2}$$

The gas output from the electric proportional valve flows into the rodless chamber of the cylinder through the air pipe, and the gas flow in the pipe is equal to the gas flow at the outlet of the electric proportional valve, thus the gas flow in the pipe is expressed as

$$q = K_3(P_{in} - P_d) \tag{3}$$

$$K_3 = \rho_{av} \frac{D^2 A}{32\mu L} \tag{4}$$

In the formula, P_{in} is the pressure at the inlet of the air pipe, P_d is the pressure at the outlet of the air pipe, ρ_{av} is the average density of the gas in the pipe; D and A are the cross-sectional area and inner diameter of the pipe, respectively; μ is the viscosity coefficient.

From equation (3), the incremental model for gas flow within the air pipe can be derived:

$$\Delta q = K_3(\Delta P_{in} - \Delta P_d) \tag{5}$$

The gas finally enters the rodless chamber of the cylinder. By neglecting gas energy loss and leakage, the rate of change of gas mass flow in the system is obtained as:

$$\Delta q = \frac{dm}{dt} = \frac{d(\rho_d V_d)}{dt} \tag{6}$$

ISSN: 2710-0588

Based on the ideal gas law:

$$P_d = \rho_d R_g T_d \tag{7}$$

In the formula, P_d is the internal pressure of the rodless chamber of the cylinder, ρ_d is the gas density inside the cylinder, T_d is the thermodynamic temperature inside the cylinder, and V_d is the volume of the rodless chamber.

Assuming no heat exchange during gas flow, the relationship between the internal system temperature T and the initial temperature Ts is:

$$T = T_s \left(\frac{P_d}{P_s}\right)^{\frac{k-1}{k}} \tag{8}$$

During the working stroke, the displacement change of the cylinder rod is minimal, so the volume of gas inside the cylinder remains nearly constant. By combining equations (5) to (7), it can be obtained:

$$\Delta q = \frac{V_d}{kR_g T} \cdot \frac{dP_d}{dt} \tag{9}$$

Perform the Laplace transform on equations (2), (5), and (9) separately,

$$Q(S) = K_1 U(s) + K_2 P_{dv}(s) \tag{10}$$

$$Q(s) = K_3 P_{in}(s) - K_3 P_d(s) \tag{11}$$

$$Q(s) = \frac{V_d}{kR_g T_d} sP_d(s) \tag{12}$$

The inlet pressure of the air pipe is equal to the outlet pressure of the electro-proportional valve, and by combining the equations, it can be obtained:

$$\frac{P_d(s)}{U(s)} = \frac{K_1}{\frac{(K_3 - K_2)V_d}{kR_g T_d K_3} - K_2} \tag{13}$$

2.3. Force balance equation of the compliant grinding and polishing actuator

Perform a force analysis on the compliant grinding and polishing actuator, as shown in Figure 4.

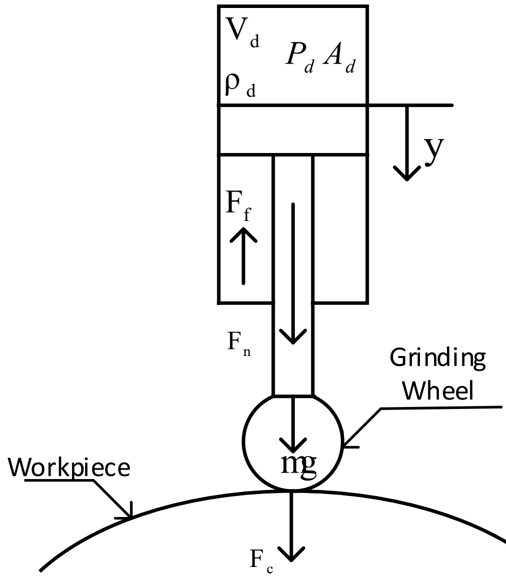

Figure 4. Force analysis diagram of the Compliant Grinding and Polishing Actuator

$$P_dA_d - P_fA_f = M\frac{d^2}{dt^2} + c_v\frac{dy}{dt} + F_n \tag{14}$$

In Figure 4, F_n is the cylinder output pressure, F_f is the actuator friction force, M is the total mass of the grinding tool, C_v is the viscous damping coefficient, and y is the extension of the cylinder piston. A low-friction cylinder is selected, and friction is ignored.P_f is the pressure in the rod chamber,A_f is the force area of the rod chamber, P_d is the pressure in the rodless chamber, and A_d is the force area of the rodless chamber. During operation, the grinding tool contacts the workpiece, generating a forceF_c, which causes the cylinder rod to displace by y. With an equivalent stiffness coefficient K_e, it follows that:

$$F_c = K_e y \tag{15}$$

Taking the Laplace transform of equations (14) and (15) and combining them yields:

$$P_d(s)A_d = Ms^2Y(s) + C_VsY(s) + F_c \tag{16}$$

$$F_c = K_eY(s) \tag{17}$$

$$\frac{F_c(s)}{P_d(s)} = \frac{K_eA_d}{Ms^2+C_vs+K_e} \tag{18}$$

The transfer function of the device can be represented as shown in Figure 5, and the system transfer function can be expressed as:

ISSN: 2710-0588

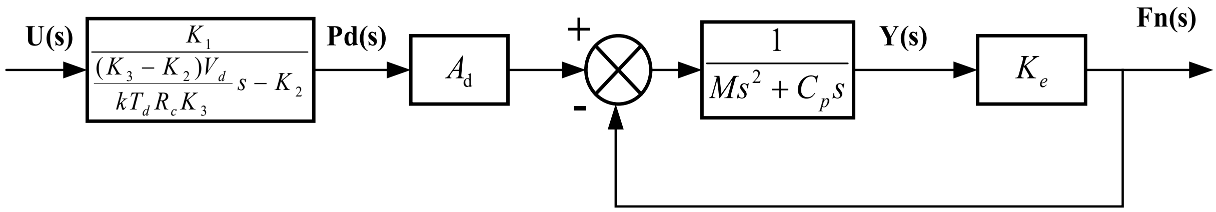

Figure 5. Transfer function block diagram of the actuato

$$G(s)=\frac{K_1K_eA_d}{\left[\frac{(K_3-K_2)V_d(s)}{kK_3R_gT_d-K_2}\right](Ms^2+k_vs+K_e)} \tag{19}$$

3. Fuzzy PID Controller Design Based on DBO Algorithm Optimization

3.1. Fuzzy PID control

The fuzzy PID adopts a two-input and three-output structure, using error e and error change rate ec as the inputs to the fuzzy controller. The outputs are the PID control parameters ΔK_p, ΔK_i, and ΔK_d. The inputs e and ec undergo fuzzy inference to output the PID controller parameters[5]. The structure of the fuzzy PID control is shown in Figure 6.

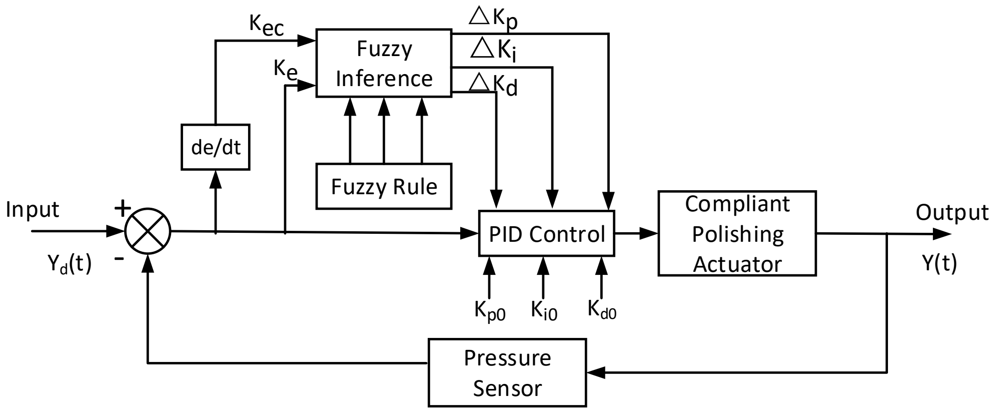

Figure 6. Structure of the fuzzy PID control

3.2. Fuzzy PID control with optimization using the dung beetle algorithm

The DBO algorithm is derived from the study of dung beetle's natural behavior. It simulates behaviors such as rolling balls, dancing, foraging, stealing, and reproduction to perform spatial search on problems according to different search strategies[6].

(1) Initialize the dung beele population and algorithm parameters: set the population size $pop = 50$, maximum iterations $M = 20$, dimension $dim = 5$, and the upper and lower bounds of the optimization variables.

(2) Calculate the Fitness Value and Update the Dung Beetle's Position: Compute the fitness value of the dung beetle based on the optimization objective, compare the existing fitness with the newly obtained fitness, and select the optimal value as the new fitness.

The optimization process of the dung beetle algorithm is as followsp:

ISSN: 2710-0588

Step1: Ball rolling. The ball-rolling dung beetle uses the sun for navigation to ensure rolling along a straight path. The position update method for the rolling dung beetle is as follows:

$$x_i(t+1) = x_i + \alpha \times k \times x_i(t-1) + b \times \Delta x$$
$$\Delta x = |x_i(t) - x^w| \tag{20}$$

In the formula, t is the current iteration number; $x_i(t)$ is the position information of the i-th dung beetle; $k \in (0, 0.2]$ is the deflection coefficient with k set to 0.1; $b \in (0, 1)$ is a natural number set to 0.3; α is a natural coefficient of 1 or -1; X^w is the global worst position; Δx simulates light intensity variation.

Step2:Dancing. When encountering an obstacle and unable to move forward, the dung beetle changes direction by dancing to find a new route. The position update is as follows:

$$x_i(t+1) = x_i + \tan(\theta)\,|x_i(t) - x_i(t-1)| \tag{21}$$

$\theta \in [0, \pi]$is the deflection angle.

Step3:Reproduction. Dung beetles choose an environment to lay eggs, using a boundary selection strategy to simulate the egg-laying area of the female:

$$Lb^* = \max(X^* \times (1-R), Lb),$$
$$Ub^* = \min(X^* \times (1+R), Ub) \tag{22}$$

X^* is the current local optimal position; $Lb^*$and $Ub^*$are the upper and lower limits of the egg-laying area; Lb and Ub are the upper and lower limits of the optimization problem; $R = 1 - t/T_{max}$, where T_{max} is the maximum number of iterations.

After determining the egg-laying area, iterations are performed, with each iteration producing an egg, i.e., a solution, and the boundaries of egg-laying change, which can prevent settling into a local optimum. The iteration process is expressed as:

$$B_i(t+1) = X^* + b_1 \times (B_i(t) - Lb^*) + b_2 \times (B_i(t) - Ub^*) \tag{23}$$

$B_i(t)$ is the position information of the i-th brooding ball at the t-th iteration; $b_1$and b_2 are two independent random vectors each with dimensions $1xD$; D is the dimension of the optimization problem.

Step4: Foraging. Juvenile dung beetles crawl out of the safe area to forage. A foraging area needs to be established to guide them, with the optimal foraging area defined as:,

$$Lb^b = \max(X^b \times (1-R), Lb)$$
$$Ub^b = \min(X^b \times (1+R), Ub) \tag{24}$$

X^b is the global optimal position; Lb and Ub are the upper and lower limits of the optimal foraging area.

Once the position constraints are set, the position updating method for the juvenile dung beetles can be defined:

$$x_i(t+1) = x_i(t) + C_1 \times (x_i - Lb^b) + C_2 \times (x_i(t) - Ub^b) \tag{25}$$

$x_i\ (t)$ is the position information of the i-th juvenile dung beetle at the t-th iteration; C_1 is a random number following a normal distribution; C_2 is a random vector within (0,1).

Step5: Stealing. X^b is the best location for food competition, thus the position update for the stealing dung beetle is as follows:

$$x_i(t+1) = X^b + S \times g \times (|x_i(t) - X^*| + |x_i(t) - X^b|) \tag{26}$$

S is a constant; g is a $1xD$ random vector that follows a normal distribution.

(3) Update the global optimal solution: Compare the fitness value of the optimal solution obtained from step (2) with the previous fitness value, and select the best value as the new fitness value.

(4) Iterative update: Repeat steps (2) and (3) until the conditions are met or the maximum number of iterations is reached, and output the optimal solution. To ensure the control system has fast performance without overshooting, the ITAE (Integral of Time-weighted Absolute Error) performance index is used as the objective evaluation function[7], with the calculation formula as follows:

$$F = \int_0^\infty t\,|e(t)|dt \tag{27}$$

The DBO algorithm is characterized by high efficiency and a balance between global and local searches. Using this algorithm, the quantization factors Ke for the error between the actual and set pressures of the compliant grinding and polishing actuator, and Kec for the rate of error change, along with the gain factors K_p, K_i, K_d of the fuzzy controller output are optimized to enhance the stability and response speed of the fuzzy PID control. The structure of the fuzzy PID control system optimized by the DBO algorithm is shown in Figure 7,

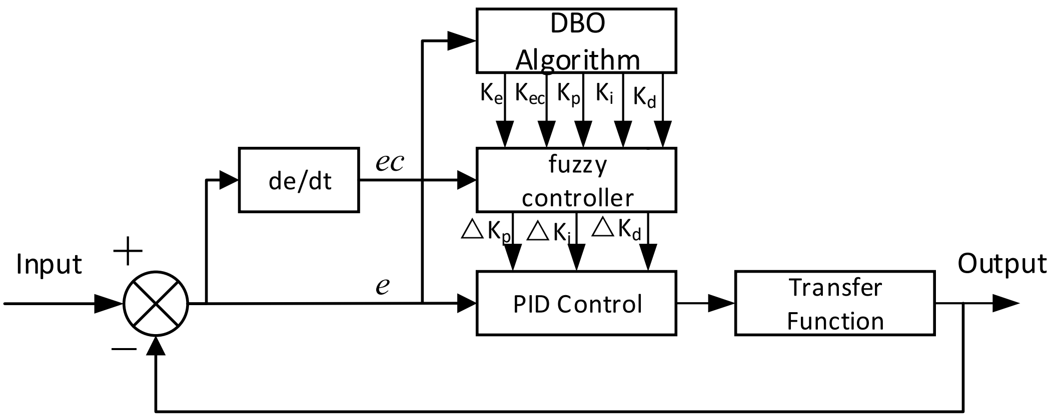

Figure 7. Structure of the fuzzy PID control system optimized by the DBO algorithm

3.3. Simulation and Result Analysis

To verify the performance of the controller, a simulation model of the compliant grinding and polishing actuator control was established using MATLAB/ Simulink module and the Fuzzy Toolbox, as shown in Figure 8.

ISSN: 2710-0588

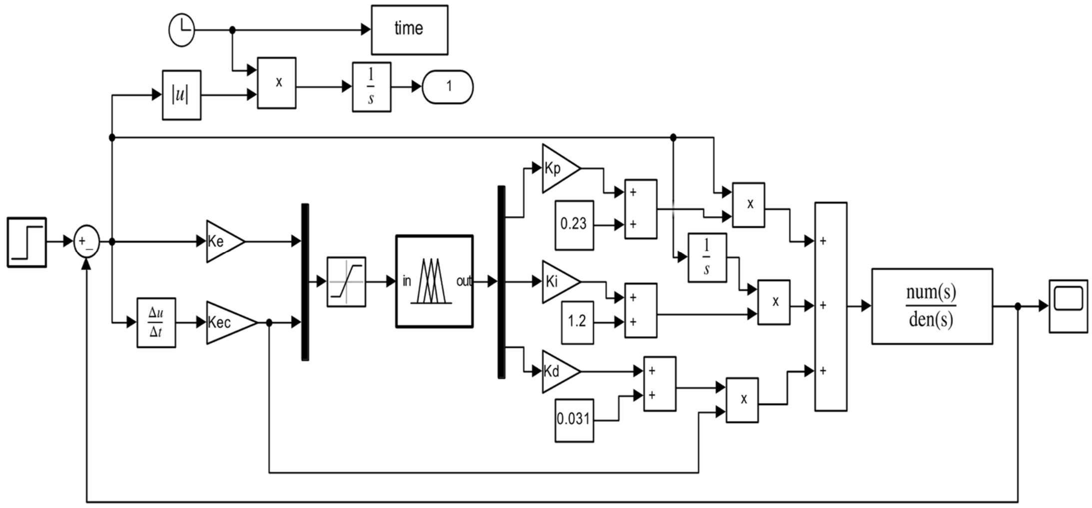

Figure 8. Fuzzy PID Control System Model Optimized by the DBO Algorithm

K_e and K_ec are the quantification factors for input error and error change rate, respectively, while K_p, K_i, K_d are the gain factors output by the fuzzy PID controller. These parameters were optimized using the DBO algorithm.

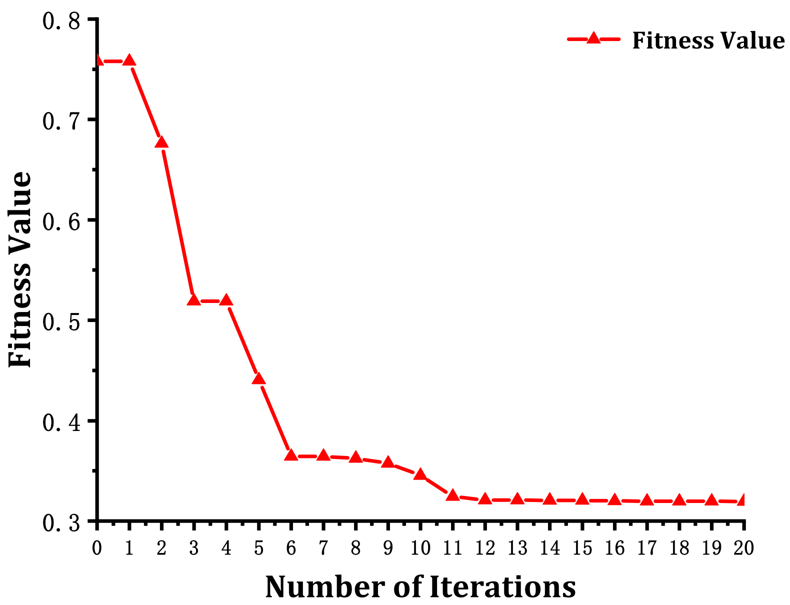

Figure 9. Iterative variation curve of the fitness value

The fitness iteration of the DBO algorithm is shown in Figure 9. After more than 13 iterations, the optimal solution is achieved, with a fitness value of 0.321.

ISSN: 2710-0588

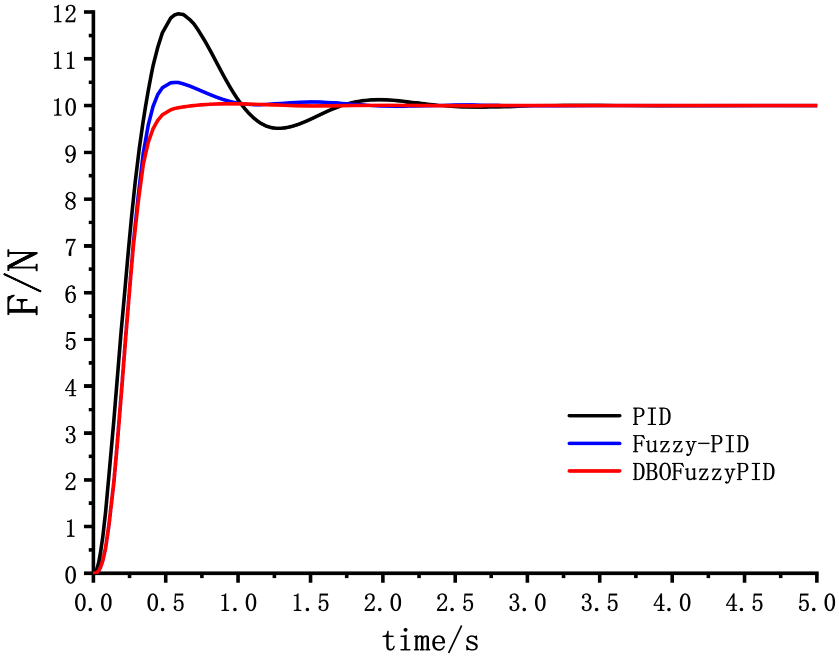

Figure 10. Response of different control methods to step signals

Figure 10 shows the response curves to a step signal using different control methods. From the comparison, it is evident that the traditional PID has significant oscillations and about 20% overshoot, stabilizing around 3 seconds with a substantial delay. The fuzzy PID, even after processing through fuzzy rules, still exhibits some overshoot and minor oscillations, stabilizing around 1.5 seconds with some response delay, and fails to eliminate the overshoot. The fuzzy PID optimized by the DBO algorithm shows no overshoot or oscillations, and has a fast response, stabilizing in about 0.5 seconds. Comparing the three, the fuzzy PID control optimized by the DBO algorithm effectively improves system response speed, reduces overshoot, and enhances system stability.

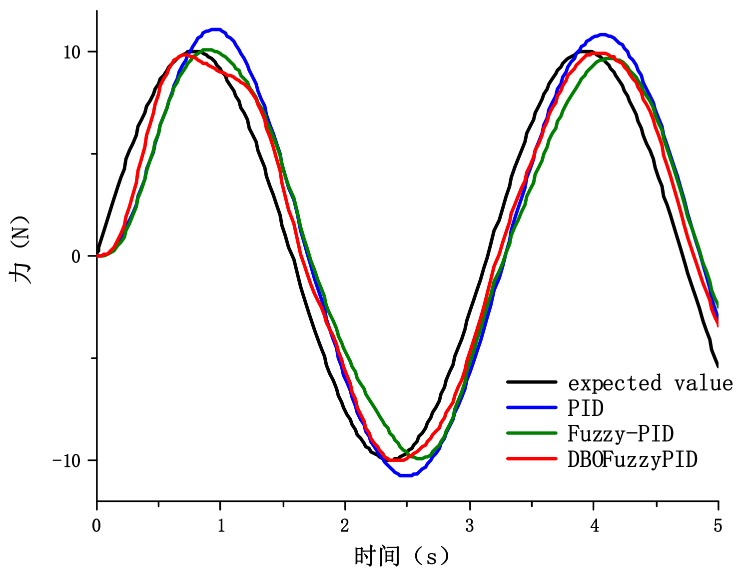

Figure 11. Sine Signal Response Curve

ISSN: 2710-0588

Figure 11 shows the simulation curves of different controllers for a sinusoidal signal. The study reveals that all three controllers exhibit certain deviations in phase and amplitude tracking. Compared to others, the PID controller has the largest deviations in both phase and amplitude. In contrast, the DBOFuzzyPID controller exhibits the lowest response curve delay at the start, enabling it to quickly track the desired command with the smallest amplitude and phase errors.

4. Conclusion

To enhance the polishing precision of robots and meet the stringent requirements for low overshoot and rapid response in the compliant polishing process, this study developed an active compliant polishing actuator that can be mounted on the end of a robot, capable of automatically adjusting the polishing pressure based on real-time changes in the polishing surface. Additionally, this paper proposes a fuzzy PID control strategy optimized using the DBO algorithm. The results indicate that, compared to traditional PID and fuzzy PID control, the fuzzy PID control optimized by the DBO algorithm not only reduces response time but also quickly achieves a stable state without overshoot, effectively enhancing system stability and response speed.

References

[1] Liang Haigang; Qiao Jinwei et al.: Analysis of Current Situation, Demand and Development Trend of Casting Grinding Technology, Micromachines, Vol.13(2022),No.19, p.1577-1577.

[2] Tie Zhang; Ye Yu, et al.: Yanbiao Zou: An Adaptive Sliding-Mode Iterative Constant-force Control Method for Robotic Belt Grinding Based on a One-Dimensional Force Sensor, Sensors, Vol 19(2019), No.7,P. 1635- 1635.

[3] Zhu D ,Feng X ,Xu X , et al.: Robotic grinding of complex components: A step towards efficient and intelligent machining – challenges, solutions, and applications, Robotics and Computer-Integrated Manufacturing, Vol 65(2020), P.1706- .

[4] Ning F, Shi Y, Cai M. et al: Research Progress of Related Technologies of Electric-Pneumatic Pressure Proportional Valves, Applied Sciences, Vol 7(2017),No.10, p.1074-1077.

[5] Szaksz Bence; Stepan Gabor: Transient chaotic behavior of fuzzy controlled polishing processes, Chaos (Woodbury, N.Y.), Vol 32(2022),No.9, p.3112-3112.

[6] Ye M ,Zhou H ,Yang H , et al.:Multi-Strategy Improved Dung Beetle Optimization Algorithm and Its Applications,Biomimetics, Vol 9(2024),No.5, p.291-.

[7] Feng T ,Deng S ,Duan Q , et al.: Application of Local Search Particle Swarm Optimization Based on the Beetle Antennae Search Algorithm in Parameter Optimization, Actuators, Vol 13(2024),No.13, p.270-270.